Polymerizing Like Mussels Do: Toward Synthetic Mussel Foot Proteins and Resistant Glues

Justus Horsch, Patrick Wilke, Matthias Pretzler, Maximilian Seuss, Inga Melnyk, Dario Remmler, Andreas Fery, Annette Rompel, and Hans G. Börner

Abstract: A novel strategy to generate adhesive protein analogues by enzyme-induced polymerization of peptides is reported. Peptide polymerization relies on tyrosinase oxidation of tyrosine residues to Dopaquinones, which rapidly form cysteinyldopa-moieties with free thiols from cysteine residues, thereby linking unimers and generating adhesive polymers. The resulting artificial protein analogues show strong adsorption to different surfaces, even resisting hypersaline conditions. Remarkable adhesion energies of up to 10.9 mJ m^{-2} are found in single adhesion events and average values are superior to those reported for mussel foot proteins that constitute the gluing interfaces.

For decades, mussel glues have offered inspiration for a variety of bio-mimetic materials.[1] Progress in understanding the mechanisms of the concerted self-assembly process of mussel foot proteins (mfps) that constitute the adhesion system led to the recognition of L-3,4-dihydroxyphenylalanine (Dopa) as a key moiety for adhesion.[2] This triggered a rich class of Dopa-carrying polymers with remarkable property profiles.[3] Dopa could either be in-built directly into polymers, leading to instant adhesives or be enzymatically generated on demand by tyrosinase processing of tyrosine-bearing precursor polymers.[4] Besides the contribution of

[*] J. Horsch, Dr. P. Wilke, D. Remmler, Prof. H. G. Börner
Laboratory for Organic Synthesis of Functional Systems
Department of Chemistry, Humboldt-Universität zu Berlin
Brook-Taylor-Straße 2, 12489 Berlin (Germany)
E-mail: h.boerner@hu-berlin.de

M. Pretzler, Prof. A. Rompel
Universität Wien, Fakultät für Chemie
Institut für Biophysikalische Chemie
Althanstraße 14, 1090 Wien (Austria)
Homepage: http://www.bpc.univie.ac.at

M. Seuss, I. Melnyk, Prof. A. Fery
Leibniz-Institut für Polymerforschung Dresden e.V.
Institute of Physical Chemistry and Polymer Physics
Hohe Straße 6, 01069 Dresden (Germany)

Prof. A. Fery
Technische Universität Dresden
Chair of Physical Chemistry of Polymeric Materials
Hohe Straße 6, 01069 Dresden (Germany)

Dopa to adhesion,[5] the role for cohesion is increasingly recognized.[6] The latter occurs either non-covalently by Fe^{3+} cross-linking of Dopa,[7] or via a set of reaction mechanisms leading to covalent Dopa cross-linking.[8] Among those is the tyrosinase-induced Michael-type addition that constitutes an exploitable pathway for the establishment of a novel polymerization process. During formation of byssal threads, polyphenol oxidase (PPO) converts L-Dopa residues in mfps into L-Dopaquinone[9] in a process that is referred to as quinone tanning. Cross-linking occurs by nucleophilic addition of protein side chain functionalities[10] and one of the most effective pathways involves cysteine addition to L-Dopaquinones.[11] Resulting cysteinyldopa cross-links are observed in various adhesive protein systems such as Pcfp-1 of *Perna canaliculus* and Mcfp-6 footprints of *Mytilus californianus*.[12]

Herein we present our study on abstracting the cysteine–dopaquinone addition from mussel adhesive systems to polymerize peptides (unimers) via tyrosinase activation. The enzyme-activated polyaddition exploits the formation of cysteinyldopa connectivities and leads to synthetic adhesive protein analogues.

The mfp-1 family constitutes a tough and flexible coating of the byssal threads. In *Mytilus edulis*, the Mefp-1 sequence contains a highly repetitive decamer AKPSYPPTYK (Figure 1).[13] Hence, polymerization of this consensus sequence might result in a polymer that resembles Mefp-1 in some aspects. To create a unimer capable of cysteinyldopa polymerization, AKPSYPPTYK was extended *C*-terminally with Cys via a tri-glycine spacer, resulting in AKPS**Y5**PP-T**Y9**KGGGC (U$_2$^{C}). Owing to the presence of two tyrosines, U$_2$^{C} would produce branched or cross-linked polymers. For ease of analysis, a linear polymer was anticipated by polymerizing a unimer that contains only Tyr9 as Tyr5 was replaced by Ser5 (AKPS**S5**PPT**Y9**KGGGC, U$_1$^{C}).

Tyrosinase occurs almost ubiquitously throughout nature, is commercially available at low cost, and meets requirements for materials science applications.[14] To avoid batch-to-batch variations,[15] the enzymatic reactions were carried out with the active form of a recombinant expressed tyrosinase (*Agaricus bisporus* polyphenol oxidase isoform 4, *Ab*PPO4).[14,16] The *Ab*PPO4 belongs to the PPO family from mushrooms and proved to practically instantaneously oxidize the tyrosine residues of U$_1$^{C} and U$_2$^{C} to Dopa and Dopaquinone as confirmed by MALDI-TOF-MS indicating species with +16 Da and +14 Da mass differences compared to non-activated unimers (Supporting Information, Figures S1, S3). More importantly, mass spectrometry as a capable tool for polymer characterization[17] proves the rapid forma-
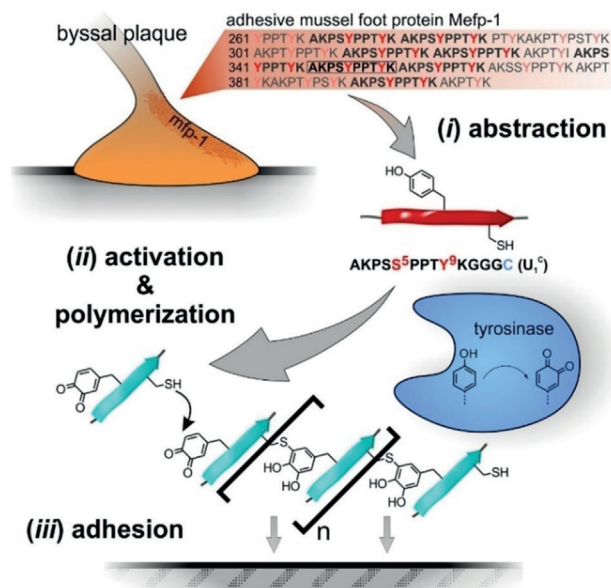
Figure 1. Principle of mussel-inspired polymerization. *i*) An amino acid sequence is abstracted from Mefp-1 and extension with Cys leads to the unimer U_1^C. *ii*) Polymerization of U_1^C can be triggered by enzymatic oxidation of tyrosine to Dopaquinone, which reacts with thiol moieties of Cys residues, enabling the formation of cysteinyldopa linkages. *iii*) The obtained mfp analogues exhibit strong adhesion to various substrates, making them useful for coatings or glues.

tion of polymerization products. MALDI-TOF-MS shows species reaching up to about 30 kDa for polyU$_1^C$ and about 25 kDa for polyU$_2^C$, which could be assigned to a degree of polymerization (DP) of up to 21 (Figure 2b). GPC analysis of polyU$_1^C$ revealed the formation of low- and high-molecular weight fractions with apparent peak molecular weights of $M_{P,app.} \approx 20$ kDa and $M_{P,app.} \approx 530$ kDa, respectively. The fractions are already present after 5–10 min and correspond to $DP_{p,app.} \approx 15$ and 260, respectively. SDS PAGE confirmed the rapid formation of species with 10–25 kDa and suggests that the polymerization appears to be completed within 10 min, as no further band shifting is observed (Supporting Information, Figure S5). The high-molecular-weight fraction found by GPC was not resolved in SDS PAGE owing to the molecular weight cut-off of the gel. Interestingly, the analysis suggests a limitation in primary polymer growth to occur at a molecular weight of about 20–25 kDa. The higher molecular weight fraction is presumably a result of subsequent cross-linking by secondary reactions such as diDopa formation (Supporting Information, Section S5.12).

For polyU$_2^C$ rather related results are observed (Supporting Information, Figure S6). Considering the additional dispersity that is caused by branching, SDS PAGE analysis shows less defined, broader bands, which reach 100 kDa, though the main band also appears at about 20–25 kDa.

MALDI-TOF-MS/MS analysis of the U_1^C polymerization mixture confirmed that the growth mechanism is based on cysteinyldopa linkages (Supporting Information, Section S5.11). The U_1^C dimer species with m/z 2722.27–2726.30 was fragmented and confirmed the presence of a cysteinyl-dopa connectivity by showing required y and b fragmentation ions. Moreover, direct proof was provided by the molecular
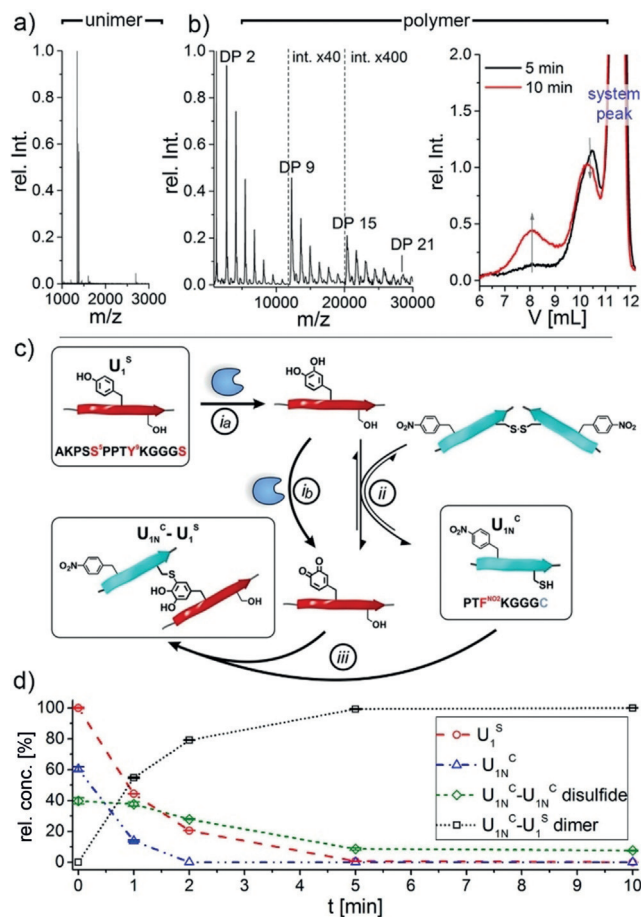

Figure 2. Enzyme-activated polymerization of U_1^C by tyrosinase to form polyU$_1^C$ (a,b) and model study revealing kinetics of tyrosinase-induced dimerization of U_1^S and U_{1N}^C (c,d). MALDI-TOF-MS of U_1^C at time zero (a) and of polyU$_1^C$ after 10 min (b, left). GPC traces of polyU$_1^C$ (b, right). c) Reaction pathway for the model dimerization shows enzymatic oxidation of tyrosine in U_1^S to Dopaquinone (*i a,b*), U_{1N}^C oxidation to disulfide by Dopaquinone reduction and the inverse reaction (*ii*) as well as U_{1N}^C-U_1^S dimer formation by cysteinyldopa linkage (*iii*). d) Relative concentrations of different species during model dimerization determined by HPLC kinetics. (Conditions: 0.25 mM of U_1^S and 0.26 mM U_{1N}^C (1/1.05, v/v) in pH 6.8 buffer, 50 U mL^{-1} *Ab*PPO4).

ions that result from the S–C$_\beta$ bond cleavage of the cysteinyldopa species.

The cross-linking reaction was investigated in a model dimerization of the monofunctional unimers AKPS**S**5PP-T**Y**9KGGG**S** (U_1^S), that contains one tyrosine but no cysteine, and PT**F**^{NO2}KGGG**C** (U_{1N}^C), which bears cysteine while tyrosine was replaced with *p*-nitrophenylalanine. The dimerization of U_1^S and U_{1N}^C occurs rapidly after enzymatic oxidation of U_1^S via cysteinyldopa formation. HPLC kinetics indicated the complete dimerization product formation within about 5 min, even at a marginal excess of U_{1N}^C (Figure 2d).

Interestingly, a secondary reaction pathway occurred leading to the formation of the disulfide bridged symmetric dimers U_{1N}^C–U_{1N}^C. The presence of redox active partners like Dopa/Dopaquinone is required to generate disulfides, as the

control reaction of $U_{1N}^C + U_1^S$ without tyrosinase has shown only 2.5 % disulfide formation after 48 h (Supporting Information, Figure S16). Thiol oxidation to disulfide can be promoted by reduction of Dopaquinone to Dopa, as has been described for the rescue protein Mcfp-6, which restores Dopa functionalities under the oxidizing seawater conditions.[18] Considering this remarkable analogy, it is likely that the reduction of Dopaquinone leads to the formation of disulfide and Dopa (Figure 2c, reaction *ii*). Intriguingly, the $U_{1N}^C–U_{1N}^C$ dimer is not a dead end, since the redox potential of the reduction of disulfides by Dopa is close to that of the oxidation of thiol by Dopaquinone.[18] Thus, reaction *ii* remains reversible and U_{1N}^C can be regenerated to undergo the favored formation of cysteinyldopa linked $U_{1N}^C–U_1^S$ dimers and drives the polymerization (reaction *iii*). Residual disulfide corresponds to the small excess of U_{1N}^C that was used to reach equivalency of effective functional groups.

The model system was further employed to illuminate potential secondary cross-linking routes. Upon enzymatic activation of U_1^S in the absence of U_{1N}^C, no polymer was detectable by SDS PAGE. This suggests the need for cysteine to enable polymerization and confirms the lower reactivity of ε-amino groups of Lys2 and Lys10 (Supporting Information, Figure S7). However, minor amounts of the dimerization product $U_1^S–U_1^S$ were found after 1 h reaction time by MALDI-TOF-MS. ESI-LC-MS/MS confirmed the nature of the connectivity to be a 5,5′-diDopa linkage as directly associated fragment ions were observed (Supporting Information, Section S5.12). None of the y, b, c, and z ions or other fragments gave evidence for lysinyldopa links. Apparently, cysteinyldopa groups are less susceptible for further coupling reactions as no subsequent cross-linking of cysteinyldopa linked $U_1^S–U_{1N}^C$ dimers was observed in a model reaction over 48 h. Conclusively, secondary cross-linking can occur via 5,5′-diDopa formation by unreacted Dopaquinones, which proceeds slower than producing the cysteinyldopa linkages. This evidence supports the hypothesis that the polymerization is driven by cysteinyldopa formation to generate primary polymerization products. These can further cross-link via secondary reactions to form high molecular weight fractions.

One of the intriguing aspects of the polymerization is the generation of cysteinyldopa functionalities at each repeat unit, which provide catechol structures and promise high surface-binding capabilities. A quartz-crystal microbalance with dissipation (QCM-D) was used to gain insights into the adsorption behavior as well as coating stability of polyU$_1^C$ and polyU$_2^C$. Both mussel foot protein analogues show rapid adsorption from aqueous solutions onto QCM sensors, exposing either alumina or fluoropolymer surfaces (Figure 3; Supporting Information, Sections S5.13 and S5.14). Multilayer formation occurs and prevents to reach equilibrium, as it is typical for protein adsorption processes. Swelling of the polyU$_2^C$ coating on alumina is indicated by the gradual decrease in Δf during buffer rinsing (Supporting Information, Figure S30). Independent of the substrate, all of the coatings almost completely defy extensive rinsing with buffer and saline seawater equivalents (599 mM NaCl). Most impressively, the coatings withstand hypersaline conditions of 4.2 M NaCl as present in water of the Dead Sea, showing
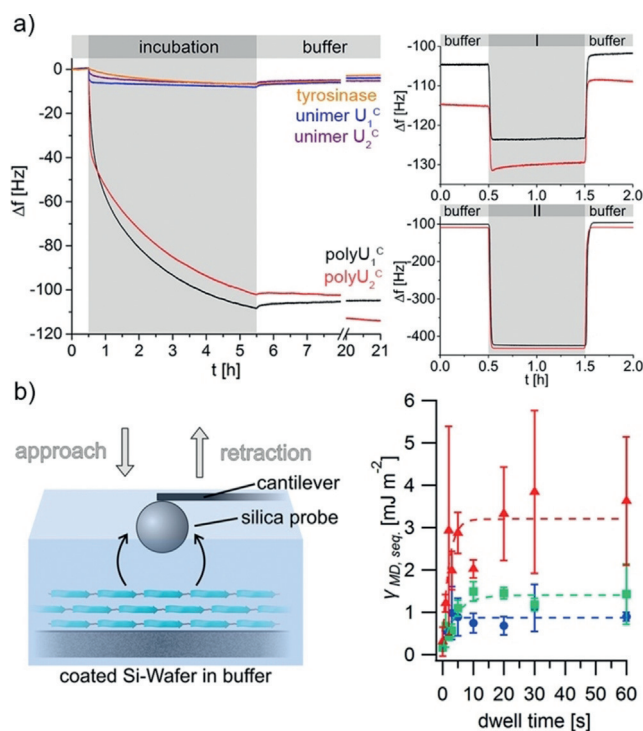

Figure 3. Adsorption (a) and adhesion (b) behavior of polyU$_1^C$ and polyU$_2^C$. a) QCM-D adsorption and desorption kinetics of mfp analogues on Al$_2$O$_3$ coated sensors (incubation step and subsequent buffer rinsing (left) and stability tests of the coatings (right) by washing with 599 mM NaCl (I) and 4.2 M hypersaline solution (II)). b) Adhesive properties of mfp analogue determined by colloidal probe AFM. Illustration of the CP-AFM contact analysis (left) and work of adhesion per unit area of polyU$_1^C$ coatings in dependence of the dwell time (right; substrates were coated for 1 h (blue), for 2 h (green) and 1 h + post-treatment with sodium ascorbate (red); constant load force of 2 nN; lines are to guide the eye only).

negligible mass losses of 1–7 %. Hence, the coating systems proved notable adhesion and robust cohesion stabilities.

QCM data evaluation, applying the Voight model for viscoelastic films,[19] enables the estimation of areal mass densities of 40 ± 5 mg m^{-2} and 30 ± 4 mg m^{-2} with corresponding layer thicknesses of 34 ± 4 nm and 26 ± 2 nm for polyU$_1^C$ and polyU$_2^C$, respectively. Using the Sauerbrey model[20] for rigid films to calculate adsorbed polymer masses leads to lower areal mass densities and thus suggests a certain viscoelasticity of the polymer films (Supporting Information, Table S4). This is supported by the fact that a pronounced frequency dependence in the Δf and ΔD response is visible for the coatings (Supporting Information, Figures S27, S35). By comparing the values of the different models it can be deduced that the polyU$_2^C$ films give more rigid coatings, since the deviation between both models is lower than for polyU$_1^C$ coatings. This can be rationalized by the different types of netpoints in the coatings: while polyU$_1^C$ shows only non-covalent interchain contacts, the branched topology of polyU$_2^C$ has instead covalent net-points that increase network rigidity. This is consistent with covalently cross-linked Mefp-1 proteins that form more rigid coatings, that better suit the Sauerbrey regime.[21] A similar trend for coatings of polyU$_1^C$ and polyU$_2^C$

with respect to masses and thicknesses on alumina surfaces is evident for coatings on fluoropolymer substrates (Supporting Information, Figure S43). The latter are known to be highly challenging for coating, on which nonetheless marine mussels can effectively adhere well.[22] Estimated areal mass densities of 31 ± 3 mg m^{-2} and 18 ± 1 mg m^{-2} (Voight model) give theoretical layer thicknesses of 26 ± 2 nm and 15 ± 1 nm for polyU$_1^C$ and polyU$_2^C$, respectively. The mass deposition kinetics onto fluoropolymer substrates are initially slightly faster than on alumina, but after 5 h of coating time the final areal mass density is lower. This can be correlated to the priming step in the film formation process. Depending on the surface, the priming involves different contacts between peptide and substrate, which will have an influence on follow-up multilayer deposition.

Ultimately, QCM-D experiments revealed that significantly different surfaces could be effectively coated, leading to stable coatings tolerant to harsh conditions. Both the cysteinyldopa connectivities and the repetitive mfp-1 consensus sequence were probably synergistically contributing to the properties, as the unimers and the enzyme alone led to negligible adsorption.

After confirming the exceptional coating behavior of the mussel foot protein analogues, the wet adhesive performance of polyU$_1^C$ and polyU$_2^C$ was investigated with colloidal probe atomic force microscopy (CP-AFM). PolyU$_1^C$ and polyU$_2^C$ were adsorbed onto passivated silicon wafers for 1 h and 2 h, respectively. Adhesive interactions of the coatings were quantified in force vs. distance measurements with a spherical silica probe of 2.4 μm radius. The probe was approached to the coated substrates, varying the maximum load (2–50 nN) and resting dwell times (0–60 s; Supporting Information, Figure S48). With increasing dwell times, the adhesion of the probe increases in a non-linear fashion for the entire sample set (Supporting Information, Figure S49; Figure 3b). This correlates with a dynamic character of the interface in the contact area. Both coating polymers will rearrange during contact, thereby optimizing adhesive interactions with the probe. As the linear polyU$_1^C$ offers higher mobility, work of adhesion at 60 s dwell time reaches higher values of 1.4 mJ m^{-2}, compared to 0.5 mJ m^{-2} for the branched and less flexible polyU$_2^C$ (Figure 3b (2 h); Supporting Information, Figure S49). The adhesion can be increased significantly to 3.6 mJ m^{-2} and 0.9 mJ m^{-2} at 60 s dwell time by applying sodium ascorbate antioxidant to the polymer coatings of polyU$_1^C$ and polyU$_2^C$. This suggests that oxidation of cysteinyldopa to quinone derivatives might occur during sample preparation and measurements, where the presence of antioxidants can regenerate the dopa functionalities. The highest single value that was observed under such conditions reached 10.9 mJ m^{-2} for polyU$_1^C$ coatings at 30 s dwell time and 20 nN load.

As expected, complex protein-based adhesives like the native mfps exhibit individual surface binding behavior and adaptation dynamics. For instance, silica adhesion of mfp-1, which is related to the synthetic polyU$_1^C$, showed only low work of adhesion of 0.1 mJ m^{-2} at pH 5.5.[23] It is remarkable that the artificial mfps provide considerably higher work of adhesion. Moreover, the specialized mfp-3 and mfp-5 that

constitute the adhesion interface of mussels, reached maximum adhesive energy values at pH 5.5 on silica of 2.99 and 2.44 mJ m^{-2} with a contact time of 60 min,[23] respectively, which are still below the average work of adhesion attained by polyU$_1^C$ after only 60 s of contact time. It has also to be noted that a complete loss of adhesive function was reported at pH 7–7.5[22] for several mfps, including mfp-1, whereas the artificial mfp analogues are able to perform at pH 6.8.

Since there is only limited adhesion data for native mfps and absolute comparison is often difficult, CP-AFM reference experiments with a commercially available protein extract from *Mytilus edulis* (Cell-Tak) were performed. The control experiments were carried out under the same conditions as for polyU$_1^C$ (Supporting Information, Figure S50). CP-AFM revealed adhesion energies in a similar range, with an average of 3.9 mJ m^{-2} after 60 s dwell time and addition of ascorbate at 2 nN load force. Considering that Cell-Tak is an adhesive optimized for neutral pH, which consists of a mixture of mfps, wherein Mefp-1 is one component, and isolated Mefp-1 showed the lowest adhesion properties in previous studies,[24] the polyU$_1^C$ performs very well. The artificial mfp analogue seems to constitute a capable mfp-1 mimic by just relying on the consensus decapeptide of Mefp-1, but still leaves room for further improvements by sequence adaptation.

In conclusion, a novel tyrosinase-activated polymerization route to mussel foot protein (mfp) analogues was introduced. Polymerization of peptide-based unimers could be achieved using cysteinyldopa linking of an analogue of the Mefp-1 consensus decapeptide. Within a few minutes, polymers with an apparent molecular weight of up to 530 kDa are generated. The resulting artificial mfp analogues show versatile adsorption and result in coatings having excellent resistance to harsh hypersaline conditions, as demonstrated by QCM-D measurements. The adhesive energies in thin-film CP-AFM studies on silica surfaces are superior to values reported from surface apparatus studies on isolated mfp-1 as well as on isolated gluing interface proteins (mfp-3 and mfp-5). Moreover, similar adhesive energy ranges are achieved as with a commercial mussel foot protein extract from *Mytilus edulis*, which is optimized for adhesion at neutral pH. The tyrosinase-induced polymerization of peptides offers facile access to artificial mfp analogues and avoids the complexity of naturally derived proteins. Next generation universal glues can be envisioned that perform effectively even under rigorous seawater conditions and adapt to a broad range of difficult surfaces.

Acknowledgements

Conflict of interest

[1] a) H. Lee, B. P. Lee, P. B. Messersmith, *Nature* **2007**, *448*, 338–341; b) B. K. Ahn, S. Das, R. Linstadt, Y. Kaufman, N. R. Martinez-Rodriguez, R. Mirshafian, E. Kesselman, Y. Talmon, B. H. Lipshutz, J. N. Israelachvili, J. H. Waite, *Nat. Commun.* **2015**, *6*, 8663; c) P. Wilke, N. Helfricht, A. Mark, G. Papastavrou, D. Faivre, H. G. Börner, *J. Am. Chem. Soc.* **2014**, *136*, 12667—12674; d) Q. Wei, K. Achazi, H. Liebe, A. Schulz, P.-L. M. Noeske, I. Grunwald, R. Haag, *Angew. Chem. Int. Ed.* **2014**, *53*, 11650–11655; *Angew. Chem.* **2014**, *126*, 11834–11840; e) H. Woehlk, J. Steinkoenig, C. Lang, L. Michalek, V. Trouillet, P. Krolla, A. S. Goldmann, L. Barner, J. P. Blinco, C. Barner-Kowollik, K. E. Fairfull-Smith, *Langmuir* **2018**, *34*, 3264–3274.
[2] J. H. Waiter, *Ann. N. Y. Acad. Sci.* **1999**, *875*, 301–309.
[3] a) E. Faure, C. Falentin-Daudré, C. Jérôme, J. Lyskawa, D. Fournier, P. Woisel, C. Detrembleur, *Prog. Polym. Sci.* **2013**, *38*, 236–270; b) B. P. Lee, P. B. Messersmith, J. N. Israelachvili, J. H. Waite, *Annu. Rev. Mater. Res.* **2011**, *41*, 99–132.
[4] a) B. P. Lee, J. L. Dalsin, P. B. Messersmith, *Biomacromolecules* **2002**, *3*, 1038–1047; b) P. Wilke, H. G. Börner, *ACS Macro Lett.* **2012**, *1*, 871–875; c) A. Lampel, S. A. McPhee, H.-A. Park, G. G. Scott, S. Humagain, D. R. Hekstra, B. Yoo, P. W. J. M. Frederix, T.-D. Li, R. R. Abzalimov, S. G. Greenbaum, T. Tuttle, C. Hu, C. J. Bettinger, R. V. Ulijn, *Science* **2017**, *356*, 1064–1068.
[5] a) D. S. Hwang, H. Zeng, Q. Lu, J. Israelachvili, J. H. Waite, *Soft Matter* **2012**, *8*, 5640–5648; b) Q. Lu, D. S. Hwang, Y. Liu, H. Zeng, *Biomaterials* **2012**, *33*, 1903–1911; c) Q. Lu, D. X. Oh, Y. Lee, Y. Jho, D. S. Hwang, H. Zeng, *Angew. Chem. Int. Ed.* **2013**, *52*, 3944–3948; *Angew. Chem.* **2013**, *125*, 4036–4040.
[6] J. H. Waite, *Comp. Biochem. Physiol. Part B* **1990**, *97*, 19–29.

[7] M. J. Harrington, A. Masic, N. Holten-Andersen, J. H. Waite, P. Fratzl, *Science* **2010**, *328*, 216–220.
[8] L. M. McDowell, L. A. Burzio, J. H. Waite, J. Schaefer, *J. Biol. Chem.* **1999**, *274*, 20293–20295.
[9] L. V. Zuccarello, *Tissue Cell* **1981**, *13*, 701–713.
[10] M. Yu, J. Hwang, T. J. Deming, *J. Am. Chem. Soc.* **1999**, *121*, 5825–5826.
[11] a) T. Kato, S. Ito, K. Fujita, *Biochim. Biophys. Acta Gen. Subj.* **1986**, *881*, 415–421; b) D. C. S. Tse, R. L. McCreery, R. N. Adams, *J. Med. Chem.* **1976**, *19*, 37–40.
[12] a) H. Zhao, J. H. Waite, *Biochemistry* **2005**, *44*, 15915–15923; b) H. Zhao, J. H. Waite, *J. Biol. Chem.* **2006**, *281*, 26150–26158.
[13] J. H. Waite, *J. Biol. Chem.* **1983**, *258*, 2911–2915.
[14] M. Pretzler, A. Bijelic, A. Rompel, *Sci. Rep.* **2017**, *7*, 1810.
[15] A. Flurkey, J. Cooksey, A. Reddy, K. Spoonmore, A. Rescigno, J. Inlow, W. H. Flurkey, *J. Agric. Food Chem.* **2008**, *56*, 4760–4768.
[16] S. G. Mauracher, C. Molitor, C. Michael, M. Kragl, A. Rizzi, A. Rompel, *Phytochemistry* **2014**, *99*, 14–25.
[17] T. S. Fischer, J. Steinkoenig, H. Woehlk, J. P. Blinco, K. Fairfull-Smith, C. Barner-Kowollik, *Polym. Chem.* **2017**, *8*, 5269–5274.
[18] S. C. T. Nicklisch, J. E. Spahn, H. Zhou, C. M. Gruian, J. H. Waite, *Biochemistry* **2016**, *55*, 2022–2030.
[19] M. V. Voinova, M. Rodahl, M. Jonson, B. Kasemo, *Phys. Scr.* **1999**, *59*, 391.
[20] G. Sauerbrey, *Z. Phys.* **1959**, *155*, 206–222.
[21] F. Höök, B. Kasemo, T. Nylander, C. Fant, K. Sott, H. Elwing, *Anal. Chem.* **2001**, *73*, 5796–5804.
[22] Q. Lin, D. Gourdon, C. Sun, N. Holten-Andersen, T. H. Anderson, J. H. Waite, J. N. Israelachvili, *Proc. Natl. Acad. Sci. USA* **2007**, *104*, 3782–3786.
[23] Q. Lu, E. Danner, J. H. Waite, J. N. Israelachvili, H. Zeng, D. S. Hwang, *J. R. Soc. Interface* **2013**, *10*, 20120759.
[24] J. Yu, Y. Kan, M. Rapp, E. Danner, W. Wei, S. Das, D. R. Miller, Y. Chen, J. H. Waite, J. N. Israelachvili, *Proc. Natl. Acad. Sci. USA* **2013**, *110*, 15680–15685.